Atmospheric Environment 245 (2021) 118016

Contents lists available at ScienceDirect

Atmospheric Environment

journal homepage: http://www.elsevier.com/locate/atmosenv

Synoptic classification of meteorological patterns and their impact on air pollution episodes and new particle formation processes in a south European air basin

Pedro Salvador[a,*], Marcos Barreiro[a], Francisco Javier Gómez-Moreno[a], Elisabeth Alonso-Blanco[a], Begoña Artíñano[a]

[a] CIEMAT, Department of Environment, Av. Complutense 40, 28040, Madrid, Spain

HIGHLIGHTS

- Synoptic Meteorological Patterns based on sea level pressure fields were obtained.
- SMP were consistent with values of meteorological parameters in the study region.
- SMP had strong influence on exceedances of PM_{10}, NO_2 and O_3 air quality standards.
- Local high-pollution episodes were strongly associated to specific SMP.
- SMP help analysing particle size distributions and identifying new particle formation.

ARTICLE INFO

Keywords:
Circulation classification techniques
Synoptic meteorological patterns
Particle size distributions
Air pollution episodes
New particle formation

ABSTRACT

A circulation classification technique based on daily sea level pressure fields was applied to classify homogeneous synoptic types in the period 2001–2019 for the Iberian Peninsula (IP). The main synoptic meteorological patterns (SMP) were thus discriminated and then validated by the analysis of meteorological variables and atmospheric stability parameters registered in the Madrid air basin in the year 2015. Then, their utility to characterize atmospheric processes like air pollution episodes or new particle formation in the study area was evaluated. Specific SMP clearly influenced wind circulations and turbulent processes at different spatial scales. At regional scale they contributed to discriminate among pollution episodes giving rise to exceedances of air quality standards for particulate matter, nitrogen dioxide and ozone at monitoring stations. For instance, two of the resulting SMP, characterized by the presence of intense high pressure systems close to the IP and strong atmospheric stability in winter and autumn, produced slightly different urban high-pollution episodes in this region. The highest mean levels of nitrogen dioxide, PM_{10} and $PM_{2.5}$ (particles lower than 10 and 2.5 μm, respectively) and of ultrafine particles number concentration registered at different urban traffic, urban background and suburban stations, happened during these specific SMP. Likewise, most new particle formation events took place during two other SMP, which mainly occurred in spring and summer. One of them was characterized by high values of solar irradiance and surface temperature, which favour nucleation processes. The highest mean levels of ozone were also registered at the urban and rural stations during this SMP. The other one represented an unusual meteorological scenario in the IP compared to the others obtained in the study, with high pressures displaced northwest producing relatively high values of surface wind speed. This fact reduced the condensation sink and favoured new particle formation in the midday period. In short, this methodology that considers a large amount of interconnected variables can be very useful for characterizing atmospheric situations that have a strong influence on atmospheric pollution processes in other regions.

* Corresponding author.
E-mail address: pedro.salvador@ciemat.es (P. Salvador).

https://doi.org/10.1016/j.atmosenv.2020.118016
Received 21 May 2020; Received in revised form 8 September 2020; Accepted 15 October 2020
Available online 16 October 2020
1352-2310/

1. Introduction

Air pollution has a great impact on human health and the environment, especially in big cities, where more than 50% of the world's population lives (United Nations, 2015). According to the World Health Organization, chronic outdoors exposure to particulate matter (PM) and gases as tropospheric ozone (O_3) or nitrogen dioxide (NO_2) contributes to the risk of developing a large number of different diseases related to respiratory or cardiovascular problems, among others. About 4.2 million premature deaths worldwide were attributed to ambient air pollution exposure in 2016 (World Health Organization, 2018). For these reasons, air quality (AQ) plans and abatement measures to reduce air pollutant emissions have been implemented in the last decades worldwide. Despite these efforts, pollutant emissions and ambient concentrations have increased in many regions, especially in developing countries (Duncan et al., 2016).

In Europe, primary emissions and precursors of secondary air pollutants from the main source sectors (road transport, energy production and industry) have fallen over large areas due to the use of cleaner fuels and the development of technology and legislation to protect AQ (European Environmental Agency, 2018). However, sudden increases of ambient air pollutants from their background levels still take place with a relatively high frequency depending on the geographical location. These events, known as high-pollution episodes, are highly conditioned not only by the emissions intensity but also by the atmospheric conditions produced under some synoptic meteorological patterns (SMP).

Proof of this is the fact that specific SMP generate long-range transport processes of air pollutants, which give rise to high-pollution episodes worldwide (Li et al., 2002; Salvador et al., 2004; Marenco et al., 2006; Kallos et al., 2007; Querol et al., 2008; Izquierdo et al., 2014). In recent years, several studies conducted in the Mediterranean region have demonstrated that synoptic atmospheric circulations play a significant role in O_3 formation and transport at the regional and continental scale (Russo et al., 2014) and in the long-range transport of African dust towards south European countries (Salvador et al., 2014; Russo et al., 2020). Valverde et al. (2015) also demonstrated that synoptic circulation contributes to explain the spatial distribution of urban and industrial NO_2 plumes in this region. Otherwise, SMP characterized by the stationary presence of high pressure systems over large areas has frequently produced typical urban high-pollution episodes in European urban areas, due to the accumulation of air pollutant emissions under highly stable atmospheric conditions (Artíñano et al., 2003; Kukkonen et al., 2005; Reizer and Juda-Rezler, 2016; Largeron and Staquet, 2016; Borge et al., 2018).

Some methodologies can be used to objectively characterize SMP. They are known as classifications of atmospheric circulation patterns or as circulation classification techniques (Philipp et al., 2014). A circulation pattern means a field of a meteorological variable describing atmospheric circulation, defined for each time instant of the analysis on a regular longitude-latitude grid. Circulation classification techniques classify a high number of circulation patterns into a smaller group of "circulation types" or "synoptic types" according to their similarity and frequency of occurrence (Rainham et al., 2005).

Circulation classification techniques have been used in many fields of the atmospheric sciences, from weather prediction to synoptic and statistical climatology (Yarnal et al., 2001; Huth et al., 2008) but less frequently in atmospheric pollution studies. Instead, air mass back-trajectories computed by numerical models have been the most frequent tool used for estimating the origin of air masses arriving at a given site and analysing their impact on air pollutant measurements registered there (Stohl, 1998 and references therein). Specific trajectory statistical methods such as cluster analysis (CA) or residence time analysis among others (Belis et al., 2019 and references therein) can help to identify potential source regions of air pollutants, which can be transported long distances towards the measurement site. However, periods of high atmospheric stability that produces the aforementioned urban high-pollution episodes, in which the surface layer is decoupled from higher tropospheric layers, are hardly characterized by back-trajectories (Belis et al., 2019). In that case classifications of atmospheric circulation patterns using sea level pressure (SLP) data fields can be very useful for discriminating stagnant meteorological conditions, associated to the presence of high pressure systems. Thus, the main goal of this study was to demonstrate the feasibility of this approach for performing a classification of atmospheric circulation patterns able to identify and characterize specific SMP for different air pollution scenarios, including high-pollution episodes. The Madrid air basin, which is located in the central region of the Iberian Peninsula (IP) was selected as a case study, due to its great metropolitan area and vehicular fleet, and the frequent occurrence of exceedances of AQ standards for several air pollutants in the last years (MITECO, 2019).

The study was organized as follows: First, SMP were obtained and identified by means of a circulation classification technique using SLP daily fields for the period 2001–2019. Next, the year 2015 was selected to demonstrate the validity of the procedure because different documented high-pollution episodes (Borge et al., 2016; Artíñano et al., 2018) and new particle formation processes (Alonso-Blanco et al., 2107) occurred in this region. Besides, a number of heterogeneous meteorological and air pollutants data sets were available for the subsequent validation process. Then, the SMP were validated by interpreting local meteorological variables registered at an instrumented tower, atmospheric stability parameters obtained from a numerical model and variations of the mixing layer height (MLH) at midday derived from radiosondes carried out in the study area this year. Finally, the circulation classification obtained was used to evaluate the impact of the SMP on the exceedances of AQ standards and characterize specific air pollution processes, such as high-pollution episodes and new particle formation, produced in this region. To this end, a comprehensive data set of levels of air pollutants registered at urban traffic, urban background, suburban and rural background monitoring sites in the Madrid air basin were obtained. Different statistical techniques (box-plots, non-parametric tests, wind-roses, polar plots and distribution fitting) were employed for their analysis. These data sets included not only regulated parameters, such as PM_{10}, $PM_{2.5}$, NO_2 and O_3 but also ultrafine particles (UFP, particles lower than 0.1 μm) size distributions and number concentrations.

It should be noted that UFP have a high impact on AQ (Brines et al., 2015) and human health (Tobías et al., 2018) but do not appear in the regulatory frameworks so far. As their mass is not relevant compared to other parameters with higher sizes such as PM_{10} and $PM_{2.5}$, their study is addressed as number concentration and size distribution. The complexity in their measurement and the gap of knowledge on their sources, chemical speciation and behaviour in urban and suburban environments has prevented their inclusion in these regulations so far (Heal et al., 2012). Since UFP number and size distributions evolve with time depending on the atmospheric conditions, among other factors, the use of SMP may help to characterize and interpret specific atmospheric processes affecting them, like nucleation events. The advantage of this novel approach to the study of UFP is that it allows for the consideration of numerous interrelated variables within a holistic framework and represents an alternative to other descriptive and statistical methods frequently used to analyse this AQ parameter (Brines et al., 2015; Alonso-Blanco et al., 2017).

2. Methodology

2.1. Study area

The Madrid air basin is located in the centre of the IP (Fig. 1). More than three million inhabitants are concentrated in its urban core (5000 persons per square kilometre), although the metropolitan area, which includes some surrounding cities, exceeds six million inhabitants. In this context, the main source contributing to the emissions of NO_x, CO and

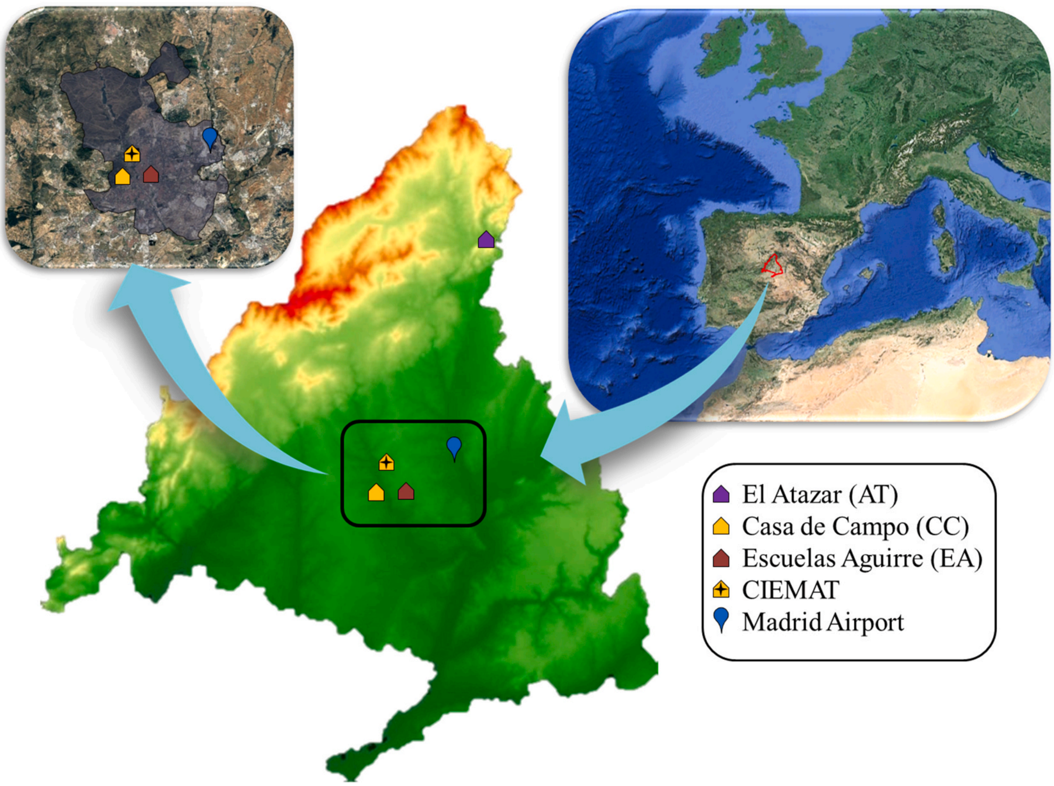

Fig. 1. Geographical location of the monitoring sites located in the Madrid air basin, and zoom to the Madrid metropolitan area (upper-left).

primary PM_{10} and $PM_{2.5}$ is road traffic with about 2 million vehicles registered in the municipality, followed by commercial, institutional and household activities (Gómez-Moreno et al., 2011; Salvador et al., 2015; Ayuntamiento de Madrid, 2017).

In this region, the NO_2 hourly limit value (200 μg/m^3 not to be exceeded more than 18 h per year) and the NO_2 annual limit value (40 μg/m^3) established in the 2008/50/EC European Directive have been systematically exceeded at many AQ urban traffic monitoring stations, since their implementation in the year 2010 (MITECO, 2019). Relatively moderate long-term average concentrations are registered in this area for some other air pollutants, such as PM_{10} and $PM_{2.5}$. However, they still reach high concentrations during the occurrence of urban high-pollution episodes (Artíñano et al., 2003; Borge et al., 2016). Moreover, it has been reported that concentration values of other pollutants, which are not commonly measured at the air quality network monitoring stations, such as PM_1, i.e. particles lower than 1 μm (Borge et al., 2016), UFP (Borge et al., 2018) or NH_3 (Artíñano et al., 2018) also experience significant increases during these episodes.

From a regional scale, the mountain breeze circulation influences the wind pattern and drives the transport of the urban plume produced over the city across the Madrid air basin. These circulations are especially relevant in summer determining the areas of impact of photochemical pollution in that period (Plaza et al., 1997; Querol et al., 2018). From a synoptic scale, there are several transboundary influences on the levels of air pollutants recorded in this geographical area. Long-range transport events of African dust, known as African dust outbreaks, frequently taking place in spring and summer, significantly increase regional background levels of PM in the Madrid air basin (Salvador et al., 2013; López et al., 2019) and consequently in its urban area (Artíñano et al., 2003; Salvador et al., 2004). Besides, air masses with a European origin occasionally transport secondary pollutants that influence their regional and urban background levels (Salvador et al., 2008; López et al., 2019). Otherwise, the arrival of Atlantic or polar air masses generally reduces drastically the levels of all air pollutants in this region (Revuelta et al., 2012).

2.2. Circulation classification methodology

The applied methodology can be described in the following steps:

First of all, SLP global fields at 12UTC derived from the National Centers for Environmental Prediction/National Centre for Atmospheric Research (NCEP/NCAR) Reanalysis dataset (Kalnay et al., 1996) provided by NOAA/OAR/ESRL PSD, USA were obtained for all the days of the period 2001–2019. SLP fields correctly describe in most of the cases, those periods characterized by stagnant meteorological conditions that give rise to urban high-pollution episodes (Pujadas et al., 2000).

Then, a non-hierarchical k-means CA method was applied for classifying the SLP daily fields, into similar groups, each one representing a prevalent circulation type (Huth et al., 2008). This is an iterative algorithm that partitions the data by comparing each object to each of the k cluster centers by a dissimilarity measurement. In this particular case, a 2.5 ° × 2.5 ° latitude – longitude regular grid centred over the IP was selected, resulting in 861 SLP grid points for each daily situation. Such grid was bounded from 20°N to 70°N and from 50°W to 50°E. The method comprises 4 stages (Belis et al., 2019):

Stage 1: an initial partitioning of the SLP fields is defined: k daily fields representing different representative synoptic meteorological situations in the study area are selected as initial seeds or cluster centers. The choices of appropriate initial clusters and their optimal number are key factors when performing a non-hierarchical k-means CA. In this study the initial cluster centers were selected from the most frequent atmospheric circulation patterns over the IP, which were identified in previous studies (Sánchez, 1993). Then, the elbow method (Kodinariya and Makwana, 2013) was used as a criterion for determining the number of clusters that will be obtained in the process.

Stage 2: calculate the change in the clustering criterion that result from changes in membership and reassign SLP fields. Hence, the euclidean distance from each field j to each cluster-centre k is calculated for every grid-point value of their 861 SLP observations and summed. Finally, the SLP field is assigned to the cluster with the smallest total distance from its cluster centre.

Stage 3: recalculate the cluster centers after all the SLP fields have been examined and assigned. The cluster centers are recalculated as the arithmetic mean of all members of any cluster.

Stage 4: repeat the steps 2 and 3 until no SLP field changes its cluster assignment.

A script in the FORTRAN programming language was created to implement the non-hierarchical k-means CA, being able to choose the initial clusters, as well as obtaining the within-group and between-group variance in the output, according to the number of clusters selected. Each resulting cluster will portray a synoptic meteorological scenario with similar properties over the centre of the IP. Once the CA was performed, composite synoptic maps were thus obtained by averaging all the SLP fields allocated in each group, grid-point by grid-point.

It should be emphasized that the non-hierarchical k-means CA procedure is one of the statistical methods most widely used for classification of atmospheric circulation patterns (Huth, 1996 and references therein; Philipp et al., 2007). Specific details on the advantage of using this method for circulation pattern classification can be found elsewhere (Huth, 1996 and references therein; Huth et al., 2008; Alonso-Pérez et al., 2011; Salvador et al., 2014; Valverde et al., 2015). However, each method removes the subjectivity inherent in classification procedures only to a certain extent. For this reason, a validation procedure on the resulting clusters was performed based on the analysis of heterogeneous data sets of meteorological variables and atmospheric stability parameters, obtained from measurements performed in an instrumented tower, numerical models and radiosondes carried out in the study region. A careful description of these databases is given below in section 2.3. This procedure pretended to assure the physical meaning of the SMP obtained from the circulation classification methodology employed in this study. Such validation process has not been usually carried out in this type of studies that used circulation classification techniques and should be considered one of the main novel features of this work.

2.3. Meteorological and atmospheric stability variables

The main variables that were used for validating the SMP resulting from the circulation classification procedure are described as follows.

Local meteorological variables were recorded in a permanent instrumented tower operating at the CIEMAT facilities (Table 1). Pressure on ground level (P), relative humidity at 4 m above ground level (agl) (HR), solar irradiance (SI) and precipitation at 35 m agl and wind speed and direction at 54 m agl (WS and WD, respectively) are currently registered with a frequency of 1 min and provided as 10 min average values. Such wind measurements were not perturbed by any obstacle, thus giving information representative of the regional wind flows produced in the air basin. The vertical difference of temperature (ΔT) was obtained as the difference of simultaneous temperature records at 54 m (upper temperature (UT)) and 4 m agl (lower temperature (LT)). Positive values of this gradient are indicative of stable atmospheric conditions that can be associated to surface thermal inversions, whereas negative values indicate atmospheric instability.

With the aim to characterize the atmospheric stability near the ground level, 3 gridded coefficients were also obtained using the mathematical routines of the HYSPLIT (HYbrid Single-Particle Lagrangian Integrated Trajectory) transport and dispersion model (Draxler et al., 1999). This model works with the ARL (Air Resources Laboratory) database of the American Agency NOAA (National Oceanic and Atmospheric Administration) for performing simulations at a particular location using gridded meteorological data. Some atmospheric stability parameters such as the subgrid-scale horizontal mixing coefficient (K_h), the vertical mixing coefficient (K_z) and the friction velocity (U*) can be obtained from them (Rolph et al., 2017). K_h is computed from the velocity deformation whereas K_z is a measure of the turbulent mixing within the boundary layer. K_z is used by this transport and dispersion model to calculate the vertical movement of pollutants, which includes the effects of both temperature and wind (thermal and mechanical turbulence). Equations used for calculation of K_h and K_z can be found in Draxler and Hess (1997) and references there in. U* is defined by the surface shear stress and the momentum flux to the surface (Britter and Hanna, 2003). The values of these stability variables were obtained at the Madrid city centre, every 3 h for any day of the year 2015 and later daily averaged.

In combination with the stability parameters, the MLH was calculated for each day of the study period by means of the simple parcel method (Holzworth, 1964) and the vertical profiles of pressure (P) and temperature (T) from radiosondes launched at 12:00 UTC in the Madrid Airport (Fig. 1 and Table 1) by the Spanish Meteorological Agency (AEMET). Taking into account that the potential temperature (θ) tends to be constant in the mixing layer, the MLH is taken as the equilibrium level of an air parcel with θ calculated at ground level. Thus, MLH was determined using this method for 351 days in 2015.

2.4. AQ data sources

Four monitoring sites that represent different but representative environmental features for AQ assessment in the Madrid air basin were chosen: CIEMAT, Escuelas Aguirre (EA), Casa de Campo (CC) and El Atazar (AT) (Fig. 1 and Table 1). The main natural and anthropogenic sources of air pollutants produce different impacts on levels registered at rural, suburban, urban background and urban traffic monitoring stations (Lenschow et al., 2001; Salvador et al., 2015; López et al., 2019). For this

Table 1
Main features of the air quality and meteorological monitoring stations and parameters analysed: P (atmospheric pressure), LT and UT (temperatures at a height of 4 and 54 m agl), SI (solar irradiance), WS (wind speed), WD (wind direction), RH (relative humidity), RAQN (Madrid Regional Air Quality Network), CAQN (Madrid City Air Quality Network), AEMET (Spanish Meteorological Agency).

Site	Coordinates	Altitude (m asl)	Type	Parameters	Temporal resolution
CIEMAT Air pollution laboratory	40°27′23″N 03°43′32″W	657	Urban background air quality levels	Particle size distribution and number concentration (15–660 nm)	4.5-min
CIEMAT Meteorological tower	40°27′23″N 03°43′28″W	680	Surface meteorological parameters	P, LT, UT, SI, WS, WD, RH, rainfall	10-min
El Atazar (AT) RAQN	40°54′32″N 03°28′04″W	995	Rural background air quality levels	PM_{10}, $PM_{2.5}$, NO_2, O_3	Hourly
Casa de Campo (CC) CAQN	40°25′10″N 03°44′50″W	645	Suburban air quality levels	PM_{10}, $PM_{2.5}$, NO_2, O_3	Hourly
Escuelas Aguirre (EA) CAQN	40°25′18″N 03°40′56″W	672	Urban traffic air quality levels	PM_{10}, $PM_{2.5}$, NO_2, O_3	Hourly
Madrid Airport AEMET	40°27′28″N 03°33′29″W	609	Vertical profiles of meteorological parameters	Vertical profiles of P and T	Daily (12:00UTC)

reason, the comparative analysis of the levels of air pollutants registered at selected stations under different synoptic atmospheric conditions can help to evaluate the influence of the SMP in AQ properties during the year 2015.

The CIEMAT research monitoring site is located in a non-residential area, in the Madrid NW city outskirts between natural forested areas and the Complutense University campus. This site is considered an urban background monitoring station because it is not directly influenced by traffic emission sources. Depending on the wind direction it is locally influenced by urban emissions from the NE-SE sector (Fig. 1) and occasionally by biogenic emissions from vegetated areas from other directions. In this site, UFP size distributions and number concentrations were measured by a scanning mobility particle sizer (TSI-SMP model 3936) formed by a differential mobility analyser (DMA; TSI Inc., Model 3081), a condensation particle counter (CPC; TSI Inc., model 3775) and an electrostatic classifier (EC; TSI Inc., model 3080). It provides in-situ continuous measurements of the particle size range from 16 to 661 nm as described by Alonso-Blanco et al. (2017). This instrument is included in the European network ACTRIS (Aerosols, Clouds, and Trace gases Research Infrastructure Network) and complies with its technical QC/DQ quality control requirements (Wiedensohler et al., 2012). Besides, it has also participated in some national intercomparison exercises through the Spanish Network of Environmental DMAs - REDMAAS (Gómez-Moreno et al., 2015). Daily mean number concentration values were determined for days with at least 75% of measurements available. Finally, 81% of all possible daily mean values were obtained in 2015.

Additionally, time series of levels of NO_2, O_3, PM_{10} and $PM_{2.5}$ (the mass of particulate matter which passes through a size selective impactor inlet with a 50% efficiency cut-off at 10 μm and 2.5 μm aerodynamic diameter, respectively) registered at EA, CC and AT were obtained with hourly resolution. EA and CC, belong to the Madrid City AQ monitoring Network (CAQN). EA is an urban traffic station located in the city centre, which currently registers very high levels of pollutants influenced by the proximity to main urban roads with a great flow of vehicles. CC corresponds to a suburban background station surrounded by forested areas that presents similar environmental characteristics and at the same distance (about 3 km) from the urban core that the CIEMAT site. Since the year 2009, when deep changes were performed in the CAQN, EA and CC are the urban traffic and suburban monitoring stations, respectively that registered the highest number of AQ parameters of this network. Finally AT site was chosen among the stations that form part of the Madrid Regional AQ monitoring Network (RAQN). This is a rural background station located 60 km away from the city centre at the N-NE direction, in a natural area next to a large water reservoir. Hence, this station registers the regional background levels of air pollutants in the Madrid air basin. Daily mean values of all air pollutants, obtained for days with at least 75% of valid hourly measurements, were available for more than 90% of the days in 2015.

Finally, complementary information regarding the occurrence of African dust outbreaks during the period 2001–2019 was analysed. This information was supplied by the Spanish Ministry for the Ecological Transition (MITECO). A procedure is annually performed for evaluating the occurrence of African dust intrusions in Spanish regions and quantifying its contributions to PM_{10} and $PM_{2.5}$ levels (Escudero et al., 2007; Viana et al., 2010). This is one of the official methods recommended by the European Commission (Commission Staff Working Paper, 2011). As a result of this analysis a total of 1337 African dust episodic days were confirmed over the IP centre in 2011–2019. In this period, 45% of all the African dust episodic days in the Madrid air basin were identified in summer, 22% in spring, 21% in autumn and 12% in winter. This is the ordinary seasonal mean distribution of African dust outbreaks across central Spain, observed in other studies (Querol et al., 2004) and with a higher statistical base in Salvador et al. (2013).

2.5. Data analysis techniques

The impact of each SMP on meteorological variables, atmospheric stability parameters and levels of air pollutants was interpreted by means of the study of boxplots. Multivariate analysis was performed with the Kruskal-Wallis non-parametric test, to search for statistically significant differences between the medians of the time series of the parameters evaluated for the resulting SMP for a 95% confidence level. Besides, wind roses and polar plot diagrams were obtained using the wind time series available from the CIEMAT meteorological tower and concentrations of air pollutants registered in the AQ monitoring stations in the year 2015. Statistical tools such as Statgraphics Centurion and the R statistical software version 3.5.1 together with the OPENAIR package (Carslaw and Ropkins, 2012; Carslaw, 2015) were used to perform these analysis.

Moreover, particle size distributions and number concentrations were analysed using averages for daily periods. Besides, 4-h periods were selected as representative of different situations according previous studies (Gómez-Moreno et al., 2011; Brines et al., 2015): night period (00–04 UTC) as a background pollution scenario; morning period (05–09 UTC) to take into account the traffic peak emissions during rush hours; midday period (11–15 UTC), when it was possible to find nucleation events and ultrafine particle size growth; and evening period (17–21 UTC), an intermediate situation incorporating also a peak associated to traffic emissions. 40 available data were required for computing each 4-h period average.

The classification of the particle size distribution by modes was defined as follows: nucleation mode between 16 and 30 nm, Aitken mode between 30 and 100 nm and accumulation mode between 100 and 661 nm. Additionally, average data were fitted to lognormal distributions (Hussein et al., 2005) in order to characterize the two main modes of the observed size distributions. An important phenomenon is the new atmospheric particle formation by nucleation events. These events were identified using the methodology proposed by Dal Maso et al. (2005). They usually happen during periods with high levels of SI and a moderate particle condensation sink.

3. Results and discussion

3.1. Circulation classification

The optimum number of clusters to be retained for the analysis was selected after repeating the CA for 2 to 8 clusters. The application of the elbow technique resulted in the grouping of all the SLP daily fields into 6 clusters, each one representing similar meteorological properties in a synoptic context. Composite SLP maps representing the mean SMP resulting from each cluster are showed in Fig. 2. The main general characteristics of each SMP were summarized as follow:

SMP-1: A synoptic situation of high atmospheric stability was represented by this cluster, where high pressures over the IP caused a blockage of the entrance of air masses from marine or continental regions outside.

SMP-2: Synoptic scenario led by an anticyclone centred on the Azores Islands and a low pressure centre situated between the United Kingdom and the Scandinavian countries. Isobars were fairly spaced and the pressure centre locations suggested the predominant occurrence of smooth NW air flows entering from the Atlantic Ocean into the IP.

SMP-3: This synoptic situation was similar to the one depicted by the scenario 2 but presented closer isobars between the high pressure centre (displaced towards southern Azores Islands) and the low pressure centre (displaced towards the west of the United Kingdom). It denoted a greater speed of the air mass flows penetrating into the IP, predominantly with a western origin.

SMP-4: The resulting situation depicted two high pressure systems, one over eastern Europe and the other over the Azores Islands, and low pressures located west of Iceland. Moderate W-NW air mass flows over

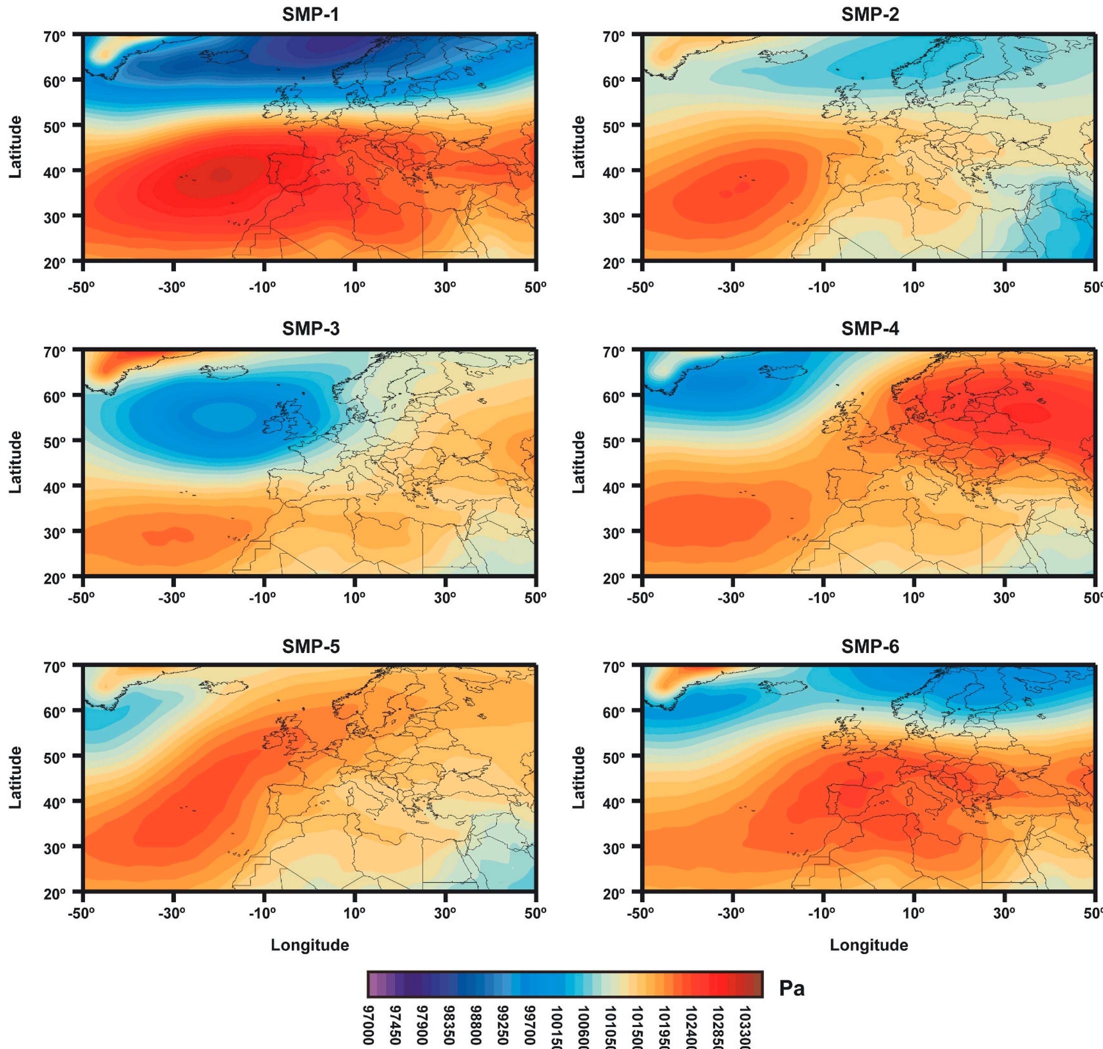

Fig. 2. Composite sea level pressure synoptic meteorological situations (Pa) for each synoptic meteorological pattern (SMP) resulting from the cluster analysis, for the period 2001–2019.

the IP should be expected under this SMP.

SMP-5: A situation with high pressures displaced northwest of the IP was determined. This SMP prevented Northern air mass flows over the IP from occurring, enabling the advection of air masses from continental Europe and the Mediterranean Sea. From this point of view it can be considered an unusual SMP, since Atlantic circulations prevails over the different regions of the IP (Querol et al., 2004, 2008).

SMP-6: This cluster showed high pressures extended along the IP, the

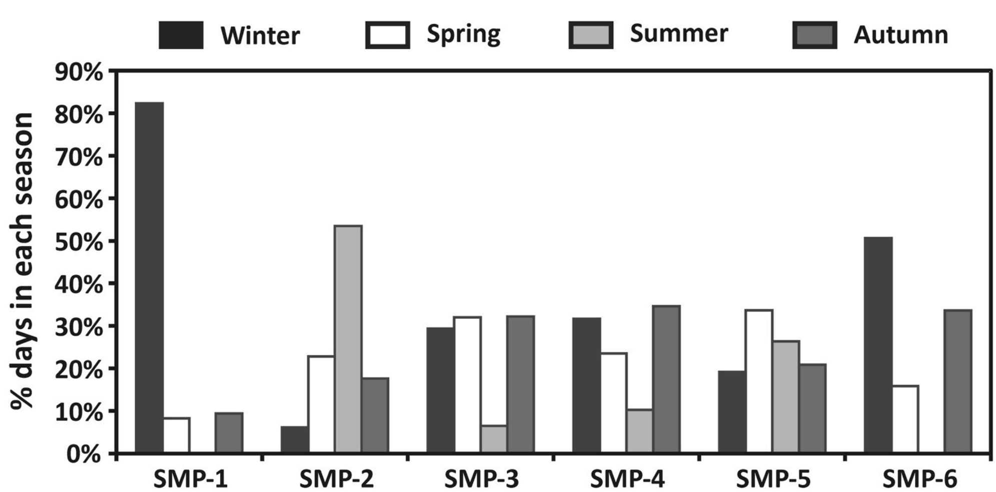

Fig. 3. Frequency of days assigned to each synoptic meteorological pattern (SMP) in the period 2001–2019.

western Mediterranean basin, France, Italy and regions of Algeria and Tunisia in the North of Africa. This situation was similar to the first scenario since both presented high pressures over the IP. Although in this case the mean pressure values were lower than in the SMP-1 and the high pressure centre was slightly displaced towards the E. This SMP coincided with "Scenario 1: NAH-S″ in the study of Escudero et al. (2005). It was one of the prevailing scenarios accounting for the occurrence of African air mass intrusions over eastern Spain during the winter and the early spring months. It is worth mentioning that most of the African dust episodic days that were detected in the winter season in this study (46%) corresponded to the SMP-6. Hence, it is found that the occurrence of SMP-6 could give rise to the transport of African dust towards the central region of the Iberian Peninsula.

The most frequent synoptic situation was the SMP-2 that took place 32% of the days of the period 2001–2019, mainly in late spring and early summer (Fig. 3). The SMP-5 also happened preferably in the spring and summer months but with a lower frequency (21% of all the days). The SMP-3 (15% of all the days) and SMP-4 (16% of all the days) were detected during all seasons but mostly in autumn and less frequently in summer. The high pressures over the IP represented by the SMP-1 (4% of all the days) and the SMP-6 (12% of all the days) exhibited a greater presence in the winter season (Fig. 3).

3.2. Validation of the SMP obtained from the circulation classification process

Daily mean values of meteorological variables and stability coefficients were analysed to characterize the local atmospheric situation represented by each synoptic pattern and thus validate the SMP obtained in the circulation classification process (Table 2). Boxplots of several meteorological and stability parameters are represented in Fig. 4.

3.2.1. Meteorological parameters

Daily averages of P and ΔT were significantly higher in SMP-1 and SMP-6 than in the other SMP (Fig. 4a and b). Besides, significantly lower daily mean values of WS, SI and LT were obtained for SMP-1 and SMP-6 than for the rest of the SMP (Fig. 4c–e). These results agreed with the high SLP gridded values over central Spain represented in Fig. 2 for SMP-1 and SMP-6 and also with the fact that most days under these SMP occurred in the winter period (Fig. 3). In this season the lowest values of SI and LT are usually reached in central Spain (AEMET, 2016). Moreover, the lowest level of accumulated rainfall was obtained for the SMP-1 (Table 2). On the contrary, the SMP with the highest frequency of occurrence in the summer months, the SMP-2 (Fig. 3) presented the highest levels of SI and LT with statistical significance (Fig. 4d and e). Otherwise, the highest statistically significant values of WS were associated to SMP-3 and SMP-5 (Fig. 4c). It is probably a consequence of the advection of relatively fast air masses of Atlantic and continental origin, respectively that happened when these circulation types occurred (Fig. 2).

3.2.2. Wind speed and direction

When it comes to the local wind pattern, it was dominated during the period of study by the NE and SW components (Figure Supplementary 1a). It followed a well-defined daily evolution characterized by a clockwise rotation during the day from NE in nocturnal and morning hours to SW in the evening period (Figure Supplementary 1b). This is the typical regional wind circulation documented in the Madrid air basin in previous studies (Plaza et al., 1997; Pujadas et al., 2000).

Additional wind roses were computed with the 10-min measurements for the days associated to each SMP (Fig. 5). As expected, the NE and SW wind directions had a great weight in the whole distribution for each SMP. However, wind direction frequencies and wind speed intensity were not the same depending on the SMP. The SMP-1, SMP-2, SMP-4 and SMP-6 presented a wind pattern similar to the one obtained for the total period, with higher winds frequencies from the NE and SW. However, unusual high wind speed from the SE direction was detected for the SMP-6 (Fig. 5). This fact could probably be produced by the southern wind flows, generated by the high pressures over the IP and the Mediterranean Sea (Fig. 2). Moreover, the SMP-3 had much more counts than usual from the third sector, because of the Atlantic synoptic circulation induced by the presence of a high and a low pressure centers in the Atlantic Ocean (Fig. 2). The SMP-1 showed the lowest wind speeds of all the SMP. The anticyclonic situation associated to this SMP probably caused the softening of the local wind speeds (Fig. 2). In the case of the

Table 2
Summary of statistical coefficients (mean, median, standard deviation−SD, interquartile range-IQR) of the main meteorological parameters analysed for each synoptic meteorological pattern (SMP) in 2015: LT (temperature at 4 m agl), RH (relative humidity), WS (wind speed), Rainfall (daily accumulated precipitation), P (atmospheric pressure), SI (solar irradiance), ΔT (vertical difference of temperature between 54 and 4 m agl), K_z (vertical mixing coefficient), U* (friction velocity), K_h (horizontal mixing coefficient) and MLH (mixing layer height at midday).

		LT (°C)	RH (%)	WS (m/s)	Rainfall (mm)	P (mb)	SI (W/m^2)	ΔT (°C)	K_z (m^2/s)	U* (m/s)	K_h (m^2/s)	MLH (m asl)
SMP-1	Mean	9.1	61.2	1.3	0.1	949.4	112.7	1.85	9.3	0.11	1638.0	986.0
	Median	7.9	64.0	0.9	0.0	949.5	100.0	2.00	6.1	0.10	1378.0	875.0
	SD	3.8	12.5	1.2	0.4	5.3	45.9	0.97	8.0	0.07	1220.3	269.7
	IQR	5.9	10.0	1.0	0.0	7.3	27.0	1.40	10.5	0.07	1448.0	295.0
SMP-2	Mean	20.4	43.1	2.5	0.6	938.6	236.5	0.20	34.3	0.23	9731.7	1820.6
	Median	21.8	37.5	2.1	0.0	939.0	266.0	0.10	29.0	0.22	11413.0	1760.0
	SD	8.3	18.6	1.9	2.4	4.7	86.6	0.52	18.0	0.10	4350.5	562.9
	IQR	13.3	28.0	2.6	0.0	4.8	145.0	0.40	26.3	0.10	7163.0	690.0
SMP-3	Mean	17.7	61.7	3.2	0.8	938.4	163.3	0.14	41.7	0.28	7388.0	1597.3
	Median	16.9	62.0	3.4	0.0	937.8	135.0	0.10	47.9	0.29	6882.0	1525.0
	SD	5.6	18.4	1.8	1.9	4.2	91.6	0.42	20.0	0.13	4060.2	410.3
	IQR	5.4	30.0	2.7	0.5	4.9	179.0	0.40	30.6	0.19	3357.0	499.0
SMP-4	Mean	15.3	53.4	2.5	0.6	940.7	169.7	0.43	27.9	0.21	5922.5	1496.0
	Median	15.4	53.0	2.2	0.0	940.1	178.0	0.30	23.4	0.20	5086.0	1404.0
	SD	7.1	17.7	1.7	2.7	4.8	73.3	0.55	17.7	0.09	3660.6	425.5
	IQR	11.6	26.0	2.2	0.0	6.3	90.0	0.70	20.2	0.10	4395.0	546.5
SMP-5	Mean	16.5	48.4	3.0	0.8	938.4	199.4	0.14	33.6	0.24	8427.6	1721.1
	Median	15.9	45.0	2.8	0.0	938.5	217.0	−0.05	31.1	0.23	8164.5	1651.0
	SD	7.8	17.9	1.9	2.3	5.0	90.2	0.61	18.8	0.10	4379.3	556.3
	IQR	13.1	21.0	2.6	0.0	6.3	152.0	0.50	27.8	0.12	7879.0	853.0
SMP-6	Mean	11.5	62.1	1.8	0.7	945.9	114.4	1.06	16.5	0.15	3000.7	1192.0
	Median	11.1	67.0	1.8	0.0	945.7	98.5	0.75	11.0	0.12	2283.0	1052.5
	SD	5.1	16.1	1.3	3.3	5.2	70.4	0.96	15.1	0.09	2537.0	454.7
	IQR	5.6	26.0	1.7	0.0	7.6	68.0	1.50	23.3	0.11	4455.0	587.0

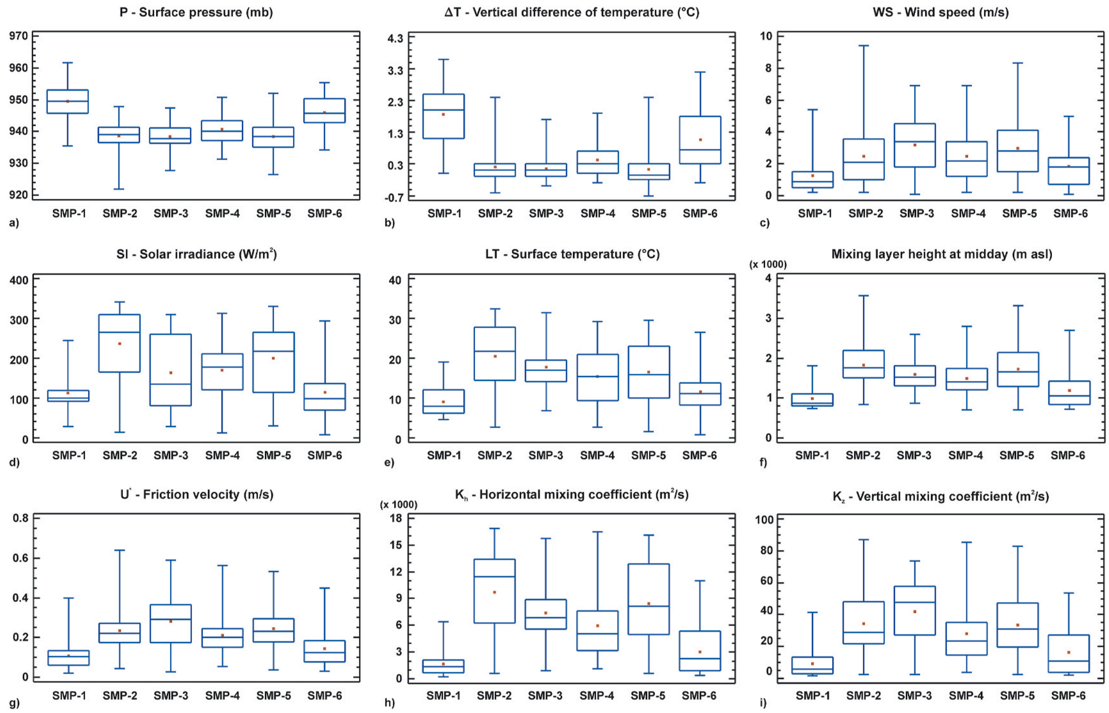

Fig. 4. Boxplots of the time series of daily mean values of the meteorological variables surface pressure (a), vertical difference of temperature (b), wind speed (c), solar irradiance (d) and surface temperature (e) measured in the CIEMAT meteorological tower and the stability parameters mixing layer height at midday (f), friction velocity (g), horizontal mixing coefficient (h) and vertical mixing coefficient (i) for the different synoptic meteorological patterns (SMP).

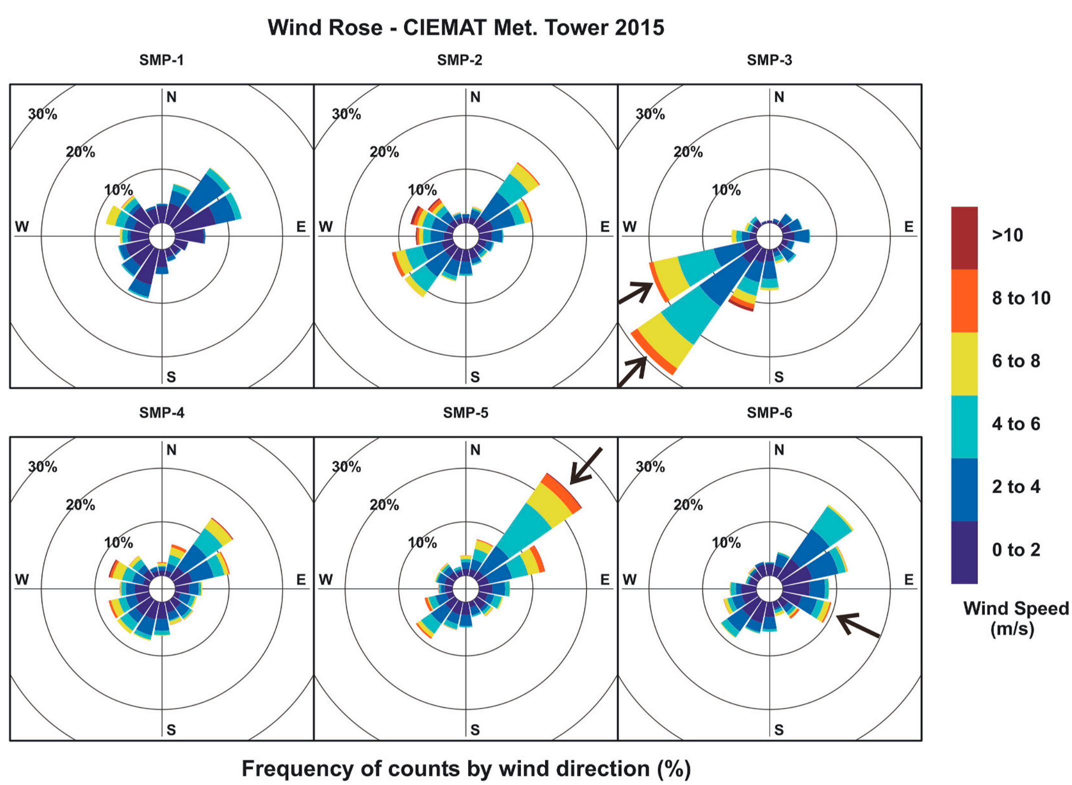

Fig. 5. Wind rose plots computed for each synoptic meteorological pattern (SMP) obtained from the wind speed and direction measurements registered at the CIEMAT meteorological tower in 2015. Black arrows highlight the main deviations from the usual regional wind cycle in the Madrid air basin, attributed to the occurrence of specific SMP.

SMP-5, the high pressures located over northern Spain increased the relative frequency of the NE winds up to 25% of the total.

3.2.3. Atmospheric stability parameters

In relation to the stability variables, statistically significant lower values of MLH, U*, K_h and K_z were obtained for SMP-1 and SMP-6 than for the other SMP (Fig. 4f–i). It means that the conditions for the dispersion of air pollutants in the Madrid air basin were lower during the occurrence of SMP-1 and SMP-6 than in the other SMP. This result is in good agreement with the high values of ΔT obtained for both SMP (Fig. 4b). The SMP-1 was the one that showed lower mean values for all the meteorological and stability variables, with the exception of ΔT for which it presented the highest mean value and less variability. This agrees with the main synoptic features of this SMP, in the sense that it included days of very high pressure and atmospheric stability over the air basin.

The highest mean values of MLH were obtained for SMP-2 and SMP-5 and to a lesser extent for SMP-3 (Fig. 4f). SMP-2 and SMP-5 presented the highest daily mean values of SI, LT and K_h (Fig. 4d and e and 4h). Otherwise, the highest daily mean records of WS, U* and K_z were obtained during days under SMP-3 and SMP-5 (Fig. 4c, g and 4i). Consequently, it could be argued that the occurrence of these SMP favoured the formation of thermal and dynamic turbulence in the low troposphere and also the vertical development of the MLH.

3.3. Assessment of the influence of the SMP on levels of air pollutants

Once the validation procedure assured the consistency and physical meaning of the SMP resulting from the circulation classification process, their influence on exceedances of AQ standards, variability of NO_2, O_3, PM_{10} and $PM_{2.5}$ concentration levels and UFP number concentrations and size distributions in the study area was carried out.

3.3.1. Exceedances of AQ standards according to different SMP

In 2015 a higher annual mean value of NO_2 was registered in EA (58 μg/m^3) than in CC (24 μg/m^3) and AT (5 μg/m^3), (Ayuntamiento de Madrid, 2015; CAM, 2019). This reduction in NO_2 concentrations was related to the distance of the monitoring AQ station to the core of the metropolitan area where road traffic emissions are usually higher (Borge et al., 2012; Salvador et al., 2015; Becerril-Valle et al., 2017). The NO_2 annual limit value was thus exceeded at EA that also exceeded the NO_2 hourly limit value in 39 occasions. Most of these exceedances were registered under the SMP-1 (20 exceedances) and SMP-6 (10 exceedances).

By contrast, the highest concentrations of O_3 were recorded in AT (82 μg/m^3) in comparison with those registered at CC (56 μg/m^3) and EA (40 μg/m^3). It is well known that O_3 levels are generally higher in rural than in urban areas. This fact was related to the transport of NO_x, which are the main anthropogenic precursors of O_3, from the Madrid Metropolitan Area towards the rural surrounding areas by the regional wind cycle and also to the presence of biogenic organic precursors in the rural environments that also favours the formation of O_3. Oppositely, NO emission titration effect in the city centers consumes O_3 in the urban areas (Plaza et al., 1997; Querol et al., 2018). The target value of O_3 for the protection of health (120 μg/m^3 as the maximum daily 8-h mean, not to be exceeded on more than 25 days/year averaged over 3 years, according to the 2008/50/EC European Directive) was exceeded in 2015 at AT (59 exceedances) and CC (56 exceedances) but not at EA (9 exceedances) (Ayuntamiento de Madrid, 2015; CAM, 2019). The information threshold for O_3 (180 μg/m^3, 2008/50/EC Directive) was also exceeded 22 h in AT and CC in the same year. Most of them happened under the SMP-2 at both sites (86% and 77% of all the exceedances in AT and CC, respectively).

When it comes to PM AQ standards, annual averaged PM_{10} and $PM_{2.5}$ concentrations measured in EA (city centre) reached 25 and 13 μg/m^3, respectively in 2015. Slightly lower values were registered in CC (19 and 10 μg/m^3, respectively) and well below levels were obtained in AT (13 and 6 μg/m^3, respectively). In 2015, these stations did not exceed either the PM_{10} (40 μg/m^3) or the $PM_{2.5}$ (25 μg/m^3) annual limit values established in the 2008/50/EC European Directive. Otherwise, the number of exceedances of the PM_{10} daily limit value (50 μg/m^3 not to be exceeded more than 35 days per year, 2008/50/EC Directive) also decreased from EA (15 exceedances) to CC (7 exceedances) and AT (2 exceedances). Most of them occurred in the July–August period and in December at the 3 monitoring stations. The most frequent synoptic situation when the exceedances happened was the SMP-6 (8 out of the 15 exceedances registered at EA). It is important to note that all the exceedances registered at CC and AT and almost all (14 out of 15) registered at EA took place during African dust episodic days. This fact is in good agreement with the occurrence of the SMP-6.

3.3.2. Variability of levels of air pollutants according to different SMP

Figs. 6 and 7 present the boxplots of the time series of PM_{10} and $PM_{2.5}$, NO_2 and O_3 levels for each SMP. Fig. 8 shows the same information for the values of daily mean UFP number concentrations registered at CIEMAT. The Kruskal–Wallis non-parametric tests indicated statistically significant differences in the levels of all the pollutants among SMP.

The highest mean levels of PM_{10} and $PM_{2.5}$ with statistical significance were obtained at the urban traffic and suburban stations for the SMP-6 closely followed by the SMP-1 (Fig. 6). Otherwise the highest statistically significant mean values of NO_2 for these stations corresponded to the SMP-1 and to a lesser extent to the SMP-6 (Fig. 7). The same result was obtained for the UFP number concentrations at the CIEMAT monitoring site (Fig. 8). These results illustrate the high levels of PM and NO_x registered during specific SMP such as the SMP-1 and the SMP-6, which favoured the accumulation of these air pollutants from the local urban sources due to the development of frequent thermal inversions, lower convective dynamics and low dispersive local circulations (Fig. 4 and Table 2). Besides, the maximum concentrations of PM_{10} and $PM_{2.5}$ that were reached in SMP-6 days at the urban sites, EA and CC were probably produced due to the additional contribution of African dust registered under many days of this SMP. Proof of it is the fact that the highest mean PM_{10} levels were also registered at the rural monitoring site during the occurrence of the SMP-6 with statistical significance. These results are in accordance with the fact showed in section 3.3.1 that most exceedances of the PM_{10} daily limit value were registered at EA, CC and AT when SMP-6 occurred. However, the mean levels of PM_{10} registered at AT during SMP-1 were lower than during the other SMP. At this rural background monitoring site mean $PM_{2.5}$ concentrations were also slightly higher in SMP-6 than in the other SMP, but differences were not statistically significant.

Moreover, the polar plot diagrams computed for the time series of PM_{10} and $PM_{2.5}$ hourly data and wind speed and direction (Figures Supplementary 2 and 3) showed that during days under SMP-1, the highest concentrations at EA and CC were registered at low wind speeds without any prevailing wind direction. However, the maximum values of PM_{10} and $PM_{2.5}$ at AT were identified with origin from the SW direction and to a lesser extent from the NE direction, associated with relatively high speeds. Hence, the origin of PM_{10} and $PM_{2.5}$ at the urban sites during SMP-1 was considered local, whereas at the rural site it had a prevailing external origin, probably associated to the regional transport of the emissions generated by the urban sources in the metropolitan area.

Otherwise, the polar plots for PM_{10} during days under the SMP-6 were quite similar at the 3 sites, showing the highest values associated to wind from the SE direction and high wind speeds (Figure Supplementary 2). Moderate PM_{10} values were identified with winds from the SW direction and high wind speeds at the 3 sites and with low wind speeds and therefore no prevailing direction at the urban traffic and suburban sites. These results probably indicated the external contribution of African dust, associated to southern wind flows, that

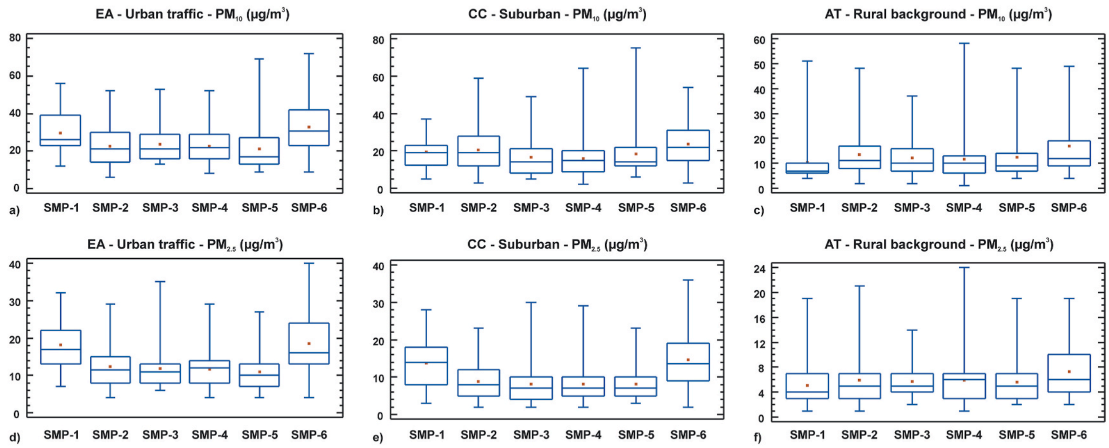

Fig. 6. Boxplots of the time series of daily mean values of PM_{10} and $PM_{2.5}$ registered during each synoptic meteorological pattern (SMP) at the urban traffic, suburban and rural background air quality monitoring stations of "Escuelas Aguirre" (EA), "Casa de Campo" (CC) and "El Atazar" (AT), respectively in the Madrid air basin during the year 2015.

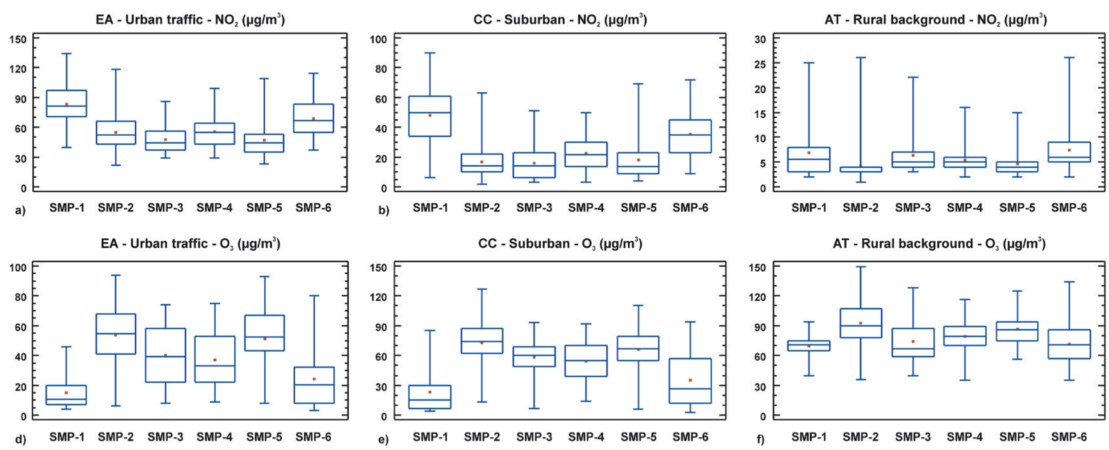

Fig. 7. Boxplots of the time series of daily mean values of NO_2 and O_3 registered during each synoptic meteorological pattern (SMP) at the urban traffic, suburban and rural background air quality monitoring stations of "Escuelas Aguirre" (EA), "Casa de Campo" (CC) and "El Atazar" (AT), respectively in the Madrid air basin during the year 2015.

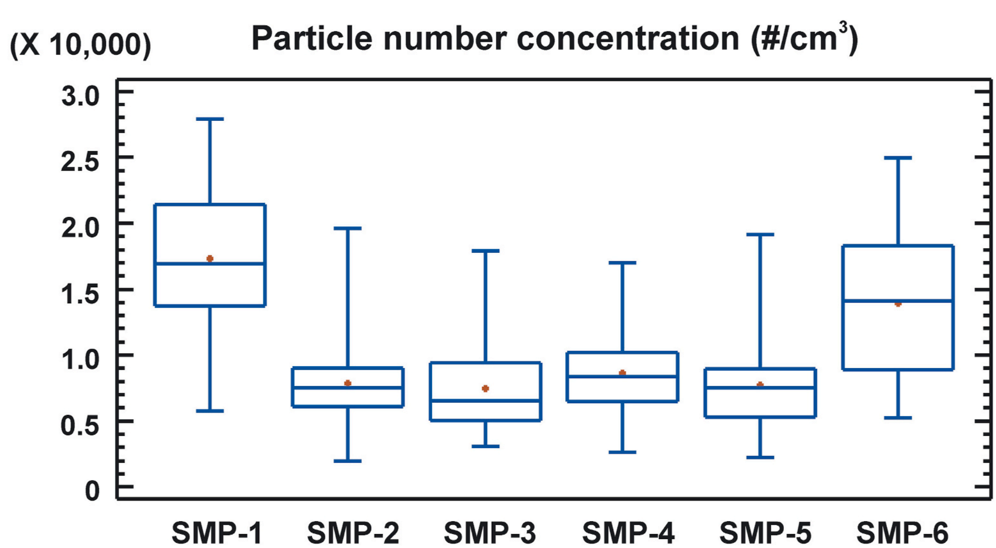

Fig. 8. Boxplots of the time series of daily mean particle number concentrations, registered during each synoptic meteorological pattern (SMP) at the urban background air quality monitoring station of "CIEMAT" during the year 2015.

increased the PM_{10} levels registered all around the Madrid air basin. In the metropolitan area, the contribution from the local sources in SMP-6 days was evidenced by the polar plots corresponding to the $PM_{2.5}$ and NO_2 time series registered in the urban monitoring sites (Figures Supplementary 3 and 4). These diagrams identified the highest concentrations for the lowest wind speeds pointing to the local sources as the main origin of the high levels of $PM_{2.5}$ and NO_2 at CC and EA during SMP-6 days. The differences obtained in the polar plots corresponding to the PM_{10} and $PM_{2.5}$ values for the SMP-6, probably are associated to the fact that African dust outbreaks generally produce a higher impact on PM_{10} than on $PM_{2.5}$ levels in the Spanish regions due to the characteristic coarse size of mineral particles in the range 2.5–10 μm (Querol et al., 2008).

It should also be mentioned that after the SMP-6 days the next highest mean levels of PM_{10} and $PM_{2.5}$ at AT were registered during the occurrence of the SMP-2 instead of the SMP-1 as at CC and EA. In the case of the time series of O_3 concentrations, statistically significant higher levels were obtained at the 3 monitoring sites during the occurrence of the SMP-2. This SMP was more frequent in the spring and summer months (Fig. 3) and had associated the highest mean levels of SI and LT (Fig. 4d and e and Table 2). These facts favour the development of photochemical reactions and illustrate the higher contribution to the regional background levels of secondary pollutants, O_3 and also secondary PM, produced under the SMP-2. Besides, the highest number of African dust episodic days in the period 2001–2019 happened during SMP-2 (44% of all days), which also contributed to increase the regional background levels of PM_{10} and to a lesser extent of $PM_{2.5}$ in the air basin.

3.3.3. Variability of UFP number concentrations and size distributions according to different SMP

Fig. 9 depicts the daily evolution of the monthly averaged particle size distributions and number concentrations along the year 2015. The annual average of the number concentration in the whole size range (16–661 nm) of the SMPS registered almost 10^4 particles per cm^3. The highest concentrations were reached during the cold months, from October to February with values higher than 3 10^4 cm^{-3} in the morning traffic peak. In these months, the highest UFP concentrations were mostly contained in the nucleation and the Aitken modes. On the contrary, the predominant peak in the period May–September was at noon, and the nucleation range was the predominant mode. It should be noted that 59 nucleation events were identified along the year, with its maximum frequency during May and June. In the present study, most nucleation events (78%) happened during SMP-2 and SMP-5, which mainly occurred in spring and summer (Fig. 3).

The annual average size distribution for every cluster is represented in Fig. 10a. The typical size distribution usually showed two peaks. The first peak was related to fresh primary emissions from traffic and could be found between 20 and 40 nm. The second peak was located around 80–100 nm, within the Aitken mode, and was related to aged particles. A possible third peak corresponding to nucleation particles could appear at the lowest detected size and grew up to 40–60 nm along a day. In these annual average distributions, all these possibilities were superimposed. Observing Fig. 10a, it was clear that the nucleation peak was almost negligible in average and the other two peaks were predominant. SMP-1 and SMP-6 showed similar distributions with an important traffic peak associated to the high stability conditions prevalent during these situations. The other SMP also showed similar distributions among them and different to those corresponding to SMP-1 and SMP-6.

When it comes to the distribution averaged for the selected day periods, Fig. 10b–e, their behaviors were similar to the general case except for the midday period, where the SMP-5 had a different pattern. For the traffic peak, this situation is closer to SMP-1 and SMP-6, while for the Aitken peak it follows the same pattern than the other clusters. The reason for this different size distribution is probably related with the fact that the SMP-5 was characterized by high values of SI and LT, which favour nucleation processes, but also of high wind speeds. Wind speed can help to produce nucleations as it clears the area reducing the condensation sink. At the same time, it can remove the semi-volatile compounds in the particles reducing their size (Alonso-Blanco et al., 2017).

Finally, it is also interesting to pay attention to the mode diameter evolution along the day for the different SMP. As already mentioned the particle size distributions were fitted to a bimodal size distribution and obtained their main characteristic parameters, including the mode diameter. In Fig. 11, this diameter was graphed for both modes and the six SMP. The traffic emissions produced a reduction in the mode diameters for all cases when comparing night to morning periods. However, in the scenarios SMP-2 to SMP-5 the diameters increased in the evening period while in SMP-1 and SMP-6 it was not so. Again, these two SMP have a different behaviour and because of the same reason, the high atmospheric stability conditions associated to their development, as it has been previously discussed.

4. Conclusions

Recent studies have highlighted the importance of characterizing the

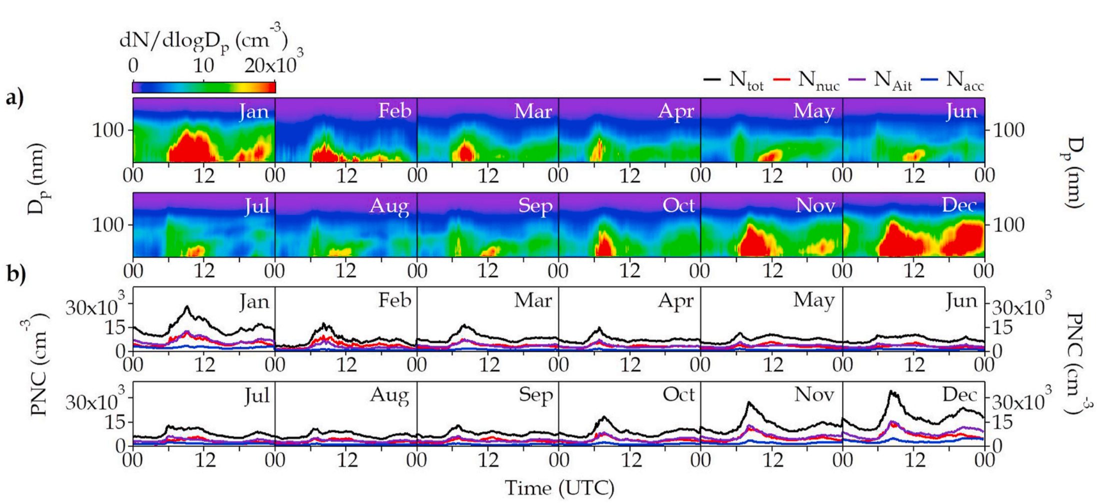

Fig. 9. Daily evolution of the monthly averaged particle size distributions (a) and particle number concentration (PNC) (b) along 2015. N_{tot} is the total number concentration for particles between particle diameters from 16 to 661 nm, N_{nuc} between 16 and 30 nm, N_{Ait} between 30 and 100 nm and N_{acc} between 100 and 661 nm.

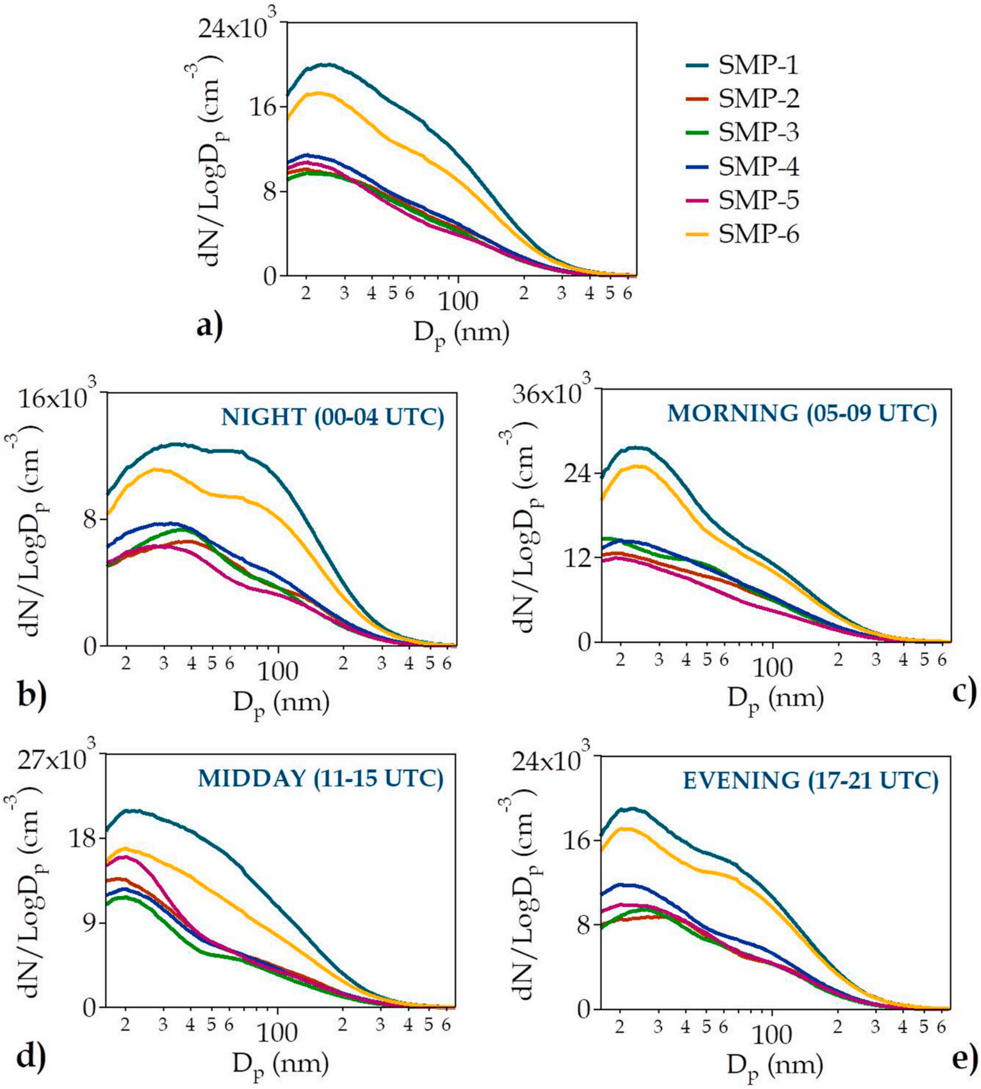

Fig. 10. Annual mean size distribution for each synoptic meteorological pattern (SMP) for the whole day (a) and the night (b), morning (c), midday (d) and evening periods of the day.

role of the synoptic circulations in the regional and local atmospheric dynamics to evaluate air quality in specific regions (Russo et al., 2014, 2020; Salvador et al., 2014; Valverde et al., 2015). In this study, more than 6900 daily SLP fields at midday for Europe and northern Africa in the period 2001–2019 were classified into 6 homogeneous SMP, though different from each other. The Madrid air basin, located in the centre of the IP, was selected as a case study. Consistency and physical meaning of the SMP were assured due to their good agreement with values of meteorological variables and atmospheric stability parameters derived from measurements carried out in an instrumented tower, numerical models and radiosondes in this region, in the year 2015. They also explained the SMP seasonal trends. Our results clearly indicate that each SMP was well characterized by wind speed and direction, even at the regional scale within the air basin, and by stability and turbulent processes that drive the vertical development of the mixing layer height. This type of validation process assures obtaining robust results from the circulation classification process, which represent the most important SMP over the region of study. Hence, it should be always carried out when evaluating circulation classifications. Other authors identified similar SMP over the western Mediterranean basin (Sánchez, 1993; Escudero et al., 2005; Valverde et al., 2015) but did not perform such validation procedure based in the analysis and interpretation of data bases of meteorological and atmospheric stability variables obtained from different sources.

The obtained SMP had a strong influence on PM_{10}, $PM_{2.5}$, NO_2 and O_3 concentrations at monitoring stations and exceedances of air quality standards could also be clearly associated to specific SMP. Non-regulated parameters such as UFP size and number distributions presented also a marked behaviour depending on the occurrence of different SMP. As far as we know, this is one of the first studies in which circulation classifications techniques have been successfully used for analysing and interpreting UFP number concentrations and size distributions.

When it comes to the development of urban high-pollution episodes, two specific SMP were identified. They were characterized by the presence of intense high pressure systems close to the IP and strong atmospheric stability in winter and autumn. The main differences between them were the magnitude and geographical location of the high pressure system. When it was located close to the western border of the IP, the highest mean levels of NO_2 and UFP number concentrations were recorded at urban and suburban monitoring stations due to the accumulation of their emissions from local sources. In the other SMP, the high pressure system was located over the IP and extended across the western Mediterranean basin and the north of Africa. In this case, NO_2

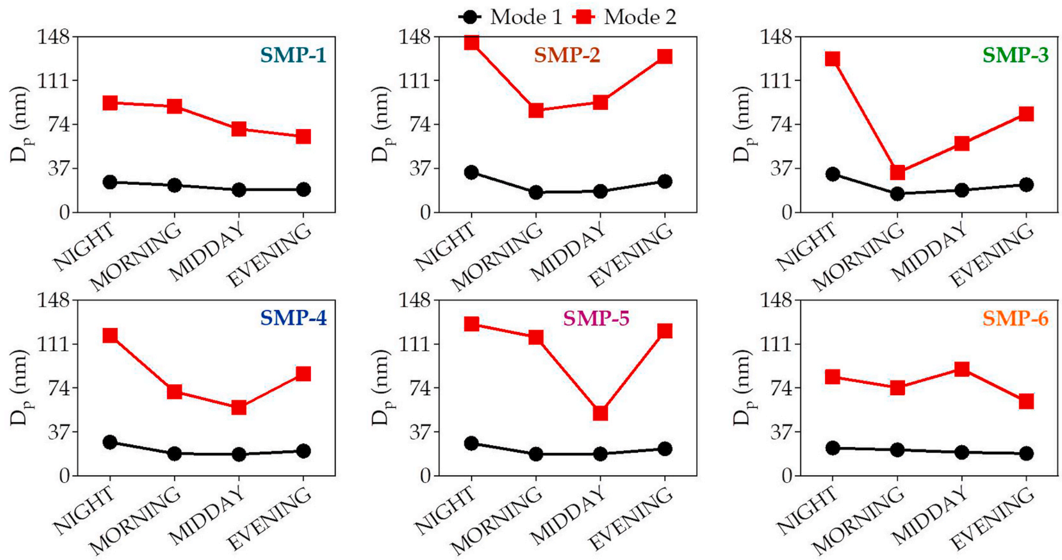

Fig. 11. Evolution of the Mode 1 (circles) and Mode 2 (squares) diameters of the particles size distributions when fitted to a bimodal size distribution for each synoptic meteorological pattern (SMP).

and UFP number concentrations were also relevant, but lower than during the former SMP, pointing to a less significant contribution of air pollutant emissions from local sources. An additional contribution of African dust, due to the favourable synoptic circulation pattern for the advection of southern air masses, gave rise to the fact that the highest mean PM_{10} and $PM_{2.5}$ values were recorded at urban, suburban and rural background stations during the occurrence of this SMP. Both SMP showed similar annual mean size distributions measured in an urban background monitoring station. An important traffic peak was detected between 20 and 40 nm, which was associated to the high stability conditions prevalent during these situations, which favour the accumulation of fresh primary emissions. Another peak that was related to aged particles was located around 80–100 nm. Since SLP maps are daily forecasted by most numerical weather prediction models that are presently used, all this information can be used for detecting and predicting future local high-pollution episodes in this region.

Moreover, most new particle formation events (78%) happened during two other SMP, which mainly occurred during spring and summer. One of them was characterized by high values of solar irradiance, surface temperature and wind speed, which favour nucleation processes. It showed an unusual mean size distribution for the midday period with a peak in the nucleation mode close to those corresponding to the SMP that gave rise to the local high-pollution episodes. The usefulness of the SMP for analyzing UFP size distributions was thus evidenced.

In this study, it has been demonstrated the utility of our novel proposal for performing classifications of atmospheric circulation patterns for characterizing unique atmospheric processes, like urban high-pollution episodes and new particle formation. It is important to stress that this kind of episodes and processes cannot be accurately identified with other techniques like atmospheric back-trajectories. In the last decade, the analysis of back-trajectories has been the most frequently used tool for characterizing atmospheric circulations and evaluating their impact in surface air quality measurements. In this work, meteorological patterns based on SLP data fields have demonstrated to be very useful for characterizing synoptic circulations and associated atmospheric conditions, and hence can be applied to different fields of the atmospheric sciences like air quality or particle formation.

CRediT authorship contribution statement

Pedro Salvador: Conceptualization, Formal analysis, Software, Resources, Investigation, Validation, Writing - original draft. **Marcos Barreiro:** Data curation, Formal analysis, Software, Resources, Visualization, Writing - review & editing. **Francisco Javier Gómez-Moreno:** Data curation, Formal analysis, Resources, Visualization, Supervision, Writing - review & editing. **Elisabeth Alonso-Blanco:** Data curation, Resources, Formal analysis, Writing - review & editing. **Begoña Artíñano:** Funding acquisition, Project administration, Supervision, Writing - review & editing.

Declaration of competing interest

The authors declare that they have no known competing financial interests or personal relationships that could have appeared to influence the work reported in this paper.

Acknowledgements

This study has been partially funded by the CRISOL Project (CGL 2017-85344-R MINECO/AEI/FEDER-UE), ACTRIS-ESPAÑA (CGL 2017-90884-REDT), TIGAS-CM (Madrid Regional Government Y2018/EMT-5177), and REDMAAS 2020 (RED 2018-102594-T). Marcos Barreiro specially acknowledges the Ministry of Science and Innovation for the predoctoral grant BES-2015-075815 associated to CIEMAT. The authors would like to thank the NOAA/OAR/ESRL PSD, Boulder, Colorado, USA for providing the sea level pressure data fields (https://psl.noaa.gov/data/). The developers of the HYSPLIT model and the NOAA-ARL READY system are also acknowledged. The authors also acknowledge the Spanish Ministry for the Ecological Transition (MITECO) for providing access to the annual files of dates of African dust episodic days that were identified over the central region of the Iberian Peninsula in 2001–2019 (https://www.miteco.gob.es/es/calidad-y-evaluacion-ambiental/temas/atmosfera-y-calidad-del-aire/calidad-del-aire/evaluacion-datos/fuentes-naturales/default.aspx).

Appendix A. Supplementary data

Supplementary data to this article can be found online at https://doi.org/10.1016/j.atmosenv.2020.118016.

References

AEMET, 2016. In: Informe Anual 2015. Ministerio de Agricultura y Pesca Alimentación y Medio Ambiente. Agencia Estatal de Meteorología Madrid 2016. NIPO: 281-16-011-

2. Technical report, pp.90. In Spanish., Available online in. https://www.aemet.es/documentos/es/conocenos/a_que_nos_dedicamos/informes/InformeAnualAEMET_2015_web.pdf. last access Sep. 2020.

Alonso-Blanco, E., Gómez-Moreno, F.J., Núñez, L., Pujadas, M., Cusack, M., Artíñano, B., 2017. Aerosol particle shrinkage event phenomenology in a South European suburban area during 2009–2015. Atmos. Environ. 160, 154–164.

Alonso-Pérez, S., Cuevas, E., Querol, X., 2011. Objective identification of synoptic meteorological patterns favouring African dust intrusions into the marine boundary layer of the subtropical eastern north Atlantic region. Meteorol. Atmos. Phys. 113 (3–4), 109.

Artíñano, B., Pujadas, M., Alonso-Blanco, E., Becerril-Valle, M., Coz, E., Gómez-Moreno, F.J., Salvador, P., Nuñez, L., Palacios, M., Díaz, E., 2018. Real-time monitoring of atmospheric ammonia during a pollution episode in Madrid (Spain). Atmos. Environ. 189, 80–88.

Artíñano, B., Salvador, P., Alonso, D.G., Querol, X., Alastuey, A., 2003. Anthropogenic and natural influence on the PM10 and PM2.5 aerosol in Madrid (Spain). Analysis of high concentration episodes. Environ. Pollut. 125 (3), 453–465.

Ayuntamiento de Madrid, 2015. Annual Air Quality Report Madrid 2015. Technical report. Dirección General de Sostenibilidad y Control Ambiental, p. 98. In Spanish., Available online. http://www.mambiente.madrid.es/opencms/export/sites/default/calaire/Anexos/Memorias/Memoria2015.pdf. last access Sep. 2020.

Ayuntamiento de Madrid, 2017. Inventory of Madrid City Air Pollutant Emissions 2017. Directorate General for Sustainability and Environmental Control. Technical report prepared by: "Fundación para el Fomento de la Innovación Industrial (F2I2) Escuela Técnica Superior de Ingenieros Industriales Technical University of Madrid (U.P. M.),". https://www.madrid.es/UnidadesDescentralizadas/Sostenibilidad/EspeInf/EnergiayCC/04CambioClimatico/4aInventario/Ficheros/EmissionsInvt2017.pdf. last access Sep. 2020.

Becerril-Valle, M., Coz, E., Prévôt, A., Močnik, G., Pandis, S., de la Campa, A.S., Alastuey, A., Díaz, E., Pérez, R., Artíñano, B., 2017. Characterization of atmospheric black carbon and co-pollutants in urban and rural areas of Spain. Atmos. Environ. 169, 36–53.

Belis, C.A., Favez, O., Mircea, M., Diapouli, E., Manousakas, M.-I., Vratolis, S., Gilardoni, S., Paglione, M., Decesari, S., Mocnik, G., Mooibroek, D., Salvador, P., Takahama, S., Vecchi, R., Paatero, P., 2019. European guide on air pollution source apportionment with receptor models - revised version 2019, EUR 29816 EN Publications Office of the European Union Luxembourg. https://doi.org/10.2760/439106,JRC117306. ISBN 978-92-76-09001-4.

Borge, R., de Miguel, I., de la Paz, D., Lumbreras, J., Pérez, J., Rodríguez, E., 2012. Comparison of road traffic emission models in Madrid (Spain). Atmos. Environ. 62, 461–471.

Borge, R., Narros, A., Artíñano, B., Yagüe, C., Gomez-Moreno, F.J., de la Paz, D., Román-Cascon, C., Díaz, E., Maqueda, G., Sastre, M., Quaassdorff, C., Dimitroulopoulou, C., Vardoulakis, S., 2016. Assessment of micro- scale spatio-temporal variation of air pollution at an urban hotspot in Madrid (Spain) through an extensive field campaign. Atmos. Environ. 140, 432–445.

Borge, R., Artíñano, B., Yagüe, C., Gomez-Moreno, F.J., Saiz-Lopez, A., Sastre, M., Narros, A., García-Nieto, D., Benavent, N., Maqueda, G., Barreiro, M., de Andrés, J. M., Cristóbal, A., 2018. Application of a short term air quality action plan in Madrid (Spain) under a high-pollution episode - Part I: diagnostic and analysis from observations. Sci. Total Environ. 635, 1561–1573.

Brines, M., Dall'Osto, M., Beddows, D.C.S., Harrison, R.M., Gómez-Moreno, F., Núñez, L., Artíñano, B., Costabile, F., Gobbi, G.P., Salimi, F., Morawska, L., Sioutas, C., Querol, X., 2015. Traffic and nucleation events as main sources of ultrafine particles in high-insolation developed world cities. Atmos. Chem. Phys. 15, 5929–5945.

Britter, R.E., Hanna, S.R., 2003. Flow and dispersion in urban areas. Annu. Rev. Fluid Mech. 35 (1), 469–496.

CAM, 2019. Annual air quality report in the Madrid community 2015, pp. 72. In: Spanish. http://gestiona.madrid.org/azul_internet/html/web/BusquedaEvaluacionAccion.icm?ESTADO_MENU=7_1. last access Sep. 2020.

Carslaw, D.C., 2015. The Open Air Manual – Open-Source Tools for Analysing Air Pollution Data. Manual for Version 1.1-4. King's College London.

Carslaw, D.C., Ropkins, K., 2012. Openair—an R package for air quality data analysis. Environ. Model. Software 27–28, 52–61.

Commission Staff Working Paper, 2011. Establishing guidelines for demonstration and subtraction of exceedances attributable to natural sources under the directive 2008/50/EC on ambient air quality and cleaner air for Europe. Brussels, 15.02.2011. SEC (2011) 208 final pp. 38. http://ec.europa.eu/environment/air/quality/legislation/pdf/sec_2011_0208.pdf. last access Sep. 2020.

Dal Maso, M., Kulmala, M., Riipinen, I., Wagner, R., Hussein, T., Aalto, P.P., Lehtinen, K. E., 2005. Formation and growth of fresh atmospheric aerosols: eight years of aerosol size distribution data from SMEAR II Hyytiala Finland. Boreal Environ. Res. 10 (5), 323.

Draxler, R.R., Hess, G., 1997. Description of the HYSPLIT_4 modelling system. In: NOAA Tech. Mem. ERL ARL-224. Sci. Rep. 28. https://www.arl.noaa.gov/documents/reports/arl-224.pdf. last access Sep. 2020.

Draxler, R.R., Stunder, B., Rolph, G., Taylor, A., 1999. HYSPLIT-4 Users's Guide, pp. 35. US Department of Commerce National Oceanic and Atmospheric Administration Environmental Research Laboratories Air Resources Laboratory.

Duncan, B.N., Lamsal, L.N., Thompson, A.M., Yoshida, Y., Lu, Z., Streets, D.G., Hurwitz, M.M., Pickering, K.E., 2016. A space-based high-resolution view of notable changes in urban NO_x pollution around the world (2005–2014). J. Geophys. Res.: Atmosphere 121 (2), 976–996.

Escudero, M., Castillo, S., Querol, X., Avila, A., Alarcón, M., Viana, M.M., Alastuey, A., Cuevas, E., Rodríguez, S., 2005. Wet and dry African dust episodes over eastern Spain. J. Geophys. Res.: Atmosphere 110, D18S08,. https://doi.org/10.1029/2004JD004731.

Escudero, M., Querol, X., Pey, J., Alastuey, A., Pérez, N., Ferreira, F., Cuevas, E., Rodríguez, S., Alonso, S., 2007. A methodology for the quantification of the net African dust load in air quality monitoring networks. Atmos. Environ. 41, 5516–5524.

European Environmental Agency, 2018. Air quality in Europe – 2018 report. EEA report Nº 12/2018, p. 83 pp. https://doi.org/10.2800/777411.

Gomez-Moreno, F.J., Pujadas, M., Plaza, J., Rodríguez-Maroto, J.J., Martínez-Lozano, P., Artíñano, B., 2011. Influence of seasonal factors on the atmospheric particle number concentration and size distribution in Madrid. Atmos. Environ. 45 (18), 3169–3180.

Gómez-Moreno, F.J., Alonso, E., Artíñano, B., Juncal-Bello, V., Iglesias-Samitier, S., Piñeiro Iglesias, M., López Mahía, P., Pérez, N., Pey, J., Ripoll, A., Alastuey, A., De La Morena, B.A., García, M.I., Rodríguez, S., Sorribas, M., Titos, G., Lyamani, H., Alados-Arboledas, L., Latorre, E., Tritscher, T., Bischof, O.F., 2015. Intercomparisons of mobility size spectrometers and condensation particle counters in the frame of the Spanish atmospheric observational aerosol network. Aerosol. Sci. Technol. 49 (9), 777–785.

Heal, M.R., Kumar, P., Harrison, R.M., 2012. Particles air quality policy and health. Chem. Soc. Rev. 41 (19), 6606–6630.

Holzworth, G.C., 1964. Estimates of mean maximum mixing depths in the contiguous United States. Mon. Weather Rev. 92 (5), 235–242.

Hussein, T., Dal Maso, M., Petäjä, T., Koponen, I.K., Paatero, P., Aalto, P.P., Hämeri, K., Kulmala, M., 2005. Evaluation of an automatic algorithm for fitting the particle number size distributions. Boreal Environ. Res. 10 (5), 337.

Huth, R., 1996. An intercomparison of computer-assisted circulation classification methods. Int. J. Climatol. 16 (8), 893–922.

Huth, R., Beck, C., Philipp, A., Demuzere, M., Ustrnul, Z., Cahynová, M., Kyselý, J., Tveito, O.E., 2008. Classifications of atmospheric circulation patterns. Ann. N. Y. Acad. Sci. 1146 (1), 105–152.

Izquierdo, R., Alarcón, M., Aguillaume, L., Ávila, A., 2014. Effects of teleconnection patterns on the atmospheric routes precipitation and deposition amounts in the north-eastern Iberian Peninsula. Atmos. Environ. 89, 482–490.

Kallos, G., Astitha, M., Katsafados, P., Spyrou, C., 2007. Long-range transport of anthropogenically and naturally produced particulate matter in the Mediterranean and North Atlantic: current state of knowledge. Journal of Applied Meteorology and Climatology 46 (8), 1230–1251.

Kalnay, E., Kanamitsu, M., Kistler, R., Collins, W., Deaven, D., Gandin, L., Iredell, M., Saha, S., White, G., Woollen, J., Zhu, Y., Chelliah, M., Ebisuzaki, W., Higgins, W., Janowiak, J., Mo, K.C., Ropelewski, C., Wang, J., Leetmaa, A., Reynolds, R., Jenne, R., Joseph, D., 1996. The NCEP/NCAR 40-year reanalysis project. Bull. Am. Meteorol. Soc. 77, 437–470.

Kodinariya, T.M., Makwana, P.R., 2013. Review on determining number of cluster in K-means clustering. International Journal of Advance Research in Computer Science and Management Studies 1 (6), 90–95.

Kukkonen, J., Pohjola, M., Sokhi, R.S., Luhana, L., Kitwiroon, N., Fragkou, L., Rantamäki, M., Berge, E., Ødegaard, V., Slørdal, L.H., Håvard, L., Denby, B., Finardi, S., 2005. Analysis and evaluation of selected local-scale PM10 air pollution episodes in four European cities: helsinki London Milan and Oslo. Atmos. Environ. 39 (15), 2759–2773.

Largeron, Y., Staquet, C., 2016. Persistent inversion dynamics and wintertime PM10 air pollution in Alpine valleys. Atmos. Environ. 135, 92–108.

Lenschow, P., Abraham, H.-J., Kutzner, K., Lutz, M., Preuß, J.-D., Reichenbächer, W., 2001. Some ideas about the sources of PM_{10}. Atmos. Environ. 35, S23–S33.

Li, Q., Jacob, D.J., Bey, I., Palmer, P.I., Duncan, B.N., Field, B.D., Martin, R.V., Fiore, A. M., Yantosca, R.M., Parrish, D.D., Simmonds, P.G., Oltmans, S.J., 2002. Transatlantic transport of pollution and its effects on surface ozone in Europe and North America. J. Geophys. Res.: Atmospheres 107(D13), ACH 4-1-ACH 4–21.

López, V., Salvador, P., Artíñano, B., Gomez-Moreno, F.J., Fernández, J., Molero, F., 2019. Influence of the origin of the air mass on the background levels of atmospheric particulate matter and secondary inorganic compounds in the Madrid air basin. Environ. Sci. Pollut. Res. 26 (29), 30426–30443.

Marenco, F., Bonasoni, P., Calzolari, F., Ceriani, M., Chiari, M., Cristofanelli, P., D'Alessandro, A., Fermo, P., Lucarelli, F., Mazzei, F., Nava, S., Piazzalunga, A., Prati, P., Valli, G., Vecchi, R., 2006. Characterization of atmospheric aerosols at Monte Cimone Italy during summer 2004: source apportionment and transport mechanisms. Journal of Geophysical Research: atmospheres 111(D24).

MITECO, 2019. Evaluación de la calidad del aire en España. Año 2018. MINISTERIO PARA LA TRANSICIÓN ECOLÓGICA. Technical report. 208 pp. In Spanish., Available online in. https://www.miteco.gob.es/es/calidad-y-evaluacion-ambiental/temas/atmosfera-y-calidad-del-aire/informeevaluacioncalidadaireespana2018_tcm30-498764.pdf last access Sep. 2020.

Philipp, A., Della-Marta, P.M., Jacobeit, J., Fereday, D.R., Jones, P.D., Moberg, A., Wanner, H., 2007. Long-term variability of daily North-Atlantic-European pressure patterns since 1850 classified by simulated annealing clustering Journal of Climate 20, 4065–4095.

Philipp, A., Beck, C., Huth, R., Jacobeit, J., 2014. Development and comparison of circulation type classifications using the COST 733 dataset and software. Int. J. Climatol. 36 (7), 2673–2691.

Plaza, J., Pujadas, M., Artíñano, B., 1997. Formation and transport of the Madrid ozone plume. J. Air Waste Manag. Assoc. 47 (7), 766–774.

Pujadas, M., Plaza, J., Terés, J., Artíñano, B., Millán, M., 2000. Passive remote sensing of nitrogen dioxide as a tool for tracking air pollution in urban areas: the Madrid urban plume a case of study. Atmos. Environ. 34 (19), 3041–3056.

Querol, X., Alastuey, A., Rodrıguez, S., Viana, M.M., Artınano, B., Salvador, P., Mantilla, E., Garcia, S., Fernandez, R., de la Rosa, J., Sánchez De La Campa, A.,

Menendez, M., Gil, J., 2004. Levels of particulate matter in rural urban and industrial sites in Spain. Sci. Total Environ. 334, 359–376.
Querol, X., Alastuey, A., Moreno, T., Viana, M.M., Castillo, S., Pey, J., Rodríguez, S., Artiñano, B., Salvador, P., Sánchez, M., Garcia Dos Santos, S., Herce Garraleta, M.D., Fernandez-Patier, R., Moreno-Grau, S., Negral, L., Minguillón, M.C., Monfort, E., Sanz, M.J., Palomo-Marín, R., Pinilla-Gil, E., Cuevas, E., de la Rosa, J., Sánchez de la Campa, A., 2008. Spatial and temporal variations in airborne particulate matter (PM10 and PM2.5) across Spain 1999–2005. Atmos. Environ. 42 (17), 3964–3979.
Querol, X., Alastuey, A., Gangoiti, G., Perez, N., Lee, H.K., Eun, H.R., Park, Y., Mantilla, E., Escudero, M., Titos, G., Alonso, L., Temime-Roussel, B., Marchand, N., Moreta, J.R., Revuelta, M.A., Salvador, P., Artíñano, B., García dos Santos, S., Anguas, M., Notario, A., Saiz-Lopez, A., Harrison, R.M., Millán, M., Ahn, K.-H., 2018. Phenomenology of summer ozone episodes over the Madrid metropolitan area central Spain. Atmos. Chem. Phys. 18, 6511–6533.
Rainham, D.G., Smoyer-Tomic, K.E., Sheridan, S.C., Burnett, R.T., 2005. Synoptic weather patterns and modification of the association between air pollution and human mortality. Int. J. Environ. Health Res. 15 (5), 347–360.
Reizer, M., Juda-Rezler, K., 2016. Explaining the high PM10 concentrations observed in Polish urban areas. Air Quality Atmosphere & Health 9 (5), 517–531.
Revuelta, M.A., Harrison, R.M., Núñez, L., Gómez Moreno, F.J., Pujadas, M., Artíñano, B., 2012. Comparison of temporal features of sulphate and nitrate at urban and rural sites in Spain and the UK. Atmos. Environ. 60, 383–391.
Rolph, G., Stein, A., Stunder, B., 2017. Real-time environmental applications and display system: Ready. Environ. Model. Software 95, 210–228.
Russo, A., Sousa, P.M., Durão, R.M., Ramos, A.M., Salvador, P., Linares, C., Díaz, J., Trigo, R.M., 2020. Saharan dust intrusions in the Iberian Peninsula: predominant synoptic conditions. Sci. Total Environ. 717, 137041.
Russo, A., Trigo, R.M., Martins, H., Mendes, M.T., 2014. NO_2, PM_{10} and O_3 urban concentrations and its association with circulation weather types in Portugal. Atmos. Environ. 89, 768–785.
Salvador, P., Alonso, D.G., Querol, X., Alastuey, A., 2004. Identification and characterisation of sources of PM10 in Madrid (Spain) by statistical methods. Atmos. Environ. 38 (3), 435–447.
Salvador, P., Artíñano, B., Querol, X., Alastuey, A., 2008. A combined analysis of backward trajectories and aerosol chemistry to characterise long-range transport episodes of particulate matter: the Madrid air basin a case study. Sci. Total Environ. 390 (2–3), 495–506.
Salvador, P., Artíñano, B., Molero, F., Viana, M.M., Pey, J., Alastuey, A., Querol, X., 2013. African dust contribution to ambient aerosol levels across central Spain: characterization of long-range transport episodes of desert dust. Atmos. Res. 127, 117–129.
Salvador, P., Alonso-Pérez, S., Pey, J., Artíñano, B., De Bustos, J.J., Alastuey, A., Querol, X., 2014. African dust outbreaks over the western Mediterranean Basin: 11-year characterization of atmospheric circulation patterns and dust source areas. Atmos. Chem. Phys. 14 (13), 6759–6775.
Salvador, P., Artíñano, B., Viana, M.M., Alastuey, A., Querol, X., 2015. Multicriteria approach to interpret the variability of the levels of particulate matter and gaseous pollutants in the Madrid metropolitan area during the 1999-2012 period. Atmos. Environ. 109, 205–216.
Sánchez, J., 1993. Situaciones atmosféricas en España. Centro de Publicaciones Ministerio de Obras Públicas. Madrid. ISBN: 84-7433-937-5. 285 pp.
Stohl, A., 1998. Computation accuracy and applications of trajectories - a review and bibliography. Atmos. Environ. 32, 947–966.
Tobías, A., Rivas, I., Reche, C., Alastuey, A., Rodríguez, S., Fernández-Camacho, R., Sánchez de la Campa, A.M., de la Rosa, J., Sunyer, J., Querol, X., 2018. Short-term effects of ultrafine particles on daily mortality by primary vehicle exhaust versus secondary origin in three Spanish cities. Environ. Int. 111, 144–155.
United Nations, 2015. Department of Economic and Social Affairs - Population Division. World Urbanization Prospects: The 2014 Revision, p. 517 (ST/ESA/SER.A/366., Available online in: https://esa.un.org/unpd/wup/publications/files/wup2014-report.pdf. last access Sep 2020).
Valverde, V., Pay, M.T., Baldasano, J.M., 2015. Circulation-type classification derived on a climatic basis to study air quality dynamics over the Iberian Peninsula. Int. J. Climatol. 35, 2877–2897.
Viana, M., Salvador, P., Artíñano, B., Querol, X., Alastuey, A., Pey, J., Latz, A.J., Cabañas, M., Moreno, T., García, S., Herce, M., Diez, P., Romero, D., Fernández, R., 2010. Assessing the performance of methods to detect and quantify African dust in airborne particulates Environmental Science & Technology 44, 8814–8820.
Wiedensohler, A., Birmili, W., Nowak, A., Sonntag, A., Weinhold, K., Merkel, M., Wehner, B., Tuch, T., Pfeifer, S., Fiebig, M., Fjäraa, A.M., Asmi, E., Sellegri, K., Depuy, R., Venzac, H., Villani, P., Laj, P., Aalto, P., Ogren, J.A., Swietlicki, E., Williams, P., Roldin, P., Quincey, P., Hüglin, C., Fierz-Schmidhauser, R., Gysel, M., Weingartner, E., Riccobono, F., Santos, S., Grüning, C., Faloon, K., Beddows, D., Harrison, R., Monahan, C., Jennings, S.G., O'Dowd, C.D., Marinoni, A., Horn, H.-G., Keck, L., Jiang, J., Scheckman, J., McMurry, P.H., Deng, Z., Zhao, C.S., Moerman, M., Henzing, B., de Leeuw, G., Löschau, G., Bastian, S., 2012. Mobility particle size spectrometers: harmonization of technical standards and data structure to facilitate high quality long-term observations of atmospheric particle number size distributions. Atmospheric Measurement Techniques 5, 657–685.
World Health Organization, 2018. World Health Statistics 2018: Monitoring Health for the SDGs Sustainable Development Goals. Licence: CC BY-NC-SA 3.0 IGO.
Yarnal, B., Comrie, A.C., Frakes, B., Brown, D.P., 2001. Developments and prospects in synoptic climatology. Int. J. Climatol. 21 (5), 1923–1950.